JOURNAL OF MATERIALS SCIENCE 20 (1985) 4215–4231

# Microstructure and phase transformations in duplex 316 submerged arc weld metal, an ageing study at 700° C

R. A. FARRAR
*Department of Mechanical Engineering, The University of Southampton, Southampton, Hampshire, UK*

The transformation of metastable $\delta$-ferrite has been studied in two duplex stainless steel weld metals. The kinetics and the nature of the equilibrium phases produced, depend upon the localized microsegregation of chromium and molybdenum to the $\delta$-ferrite laths in the as-welded state. A transformation model is proposed which suggests that a longer term stability of the $\delta$-ferrite may be achieved by alterations in the basic 316L composition used for the production of submerged arc weld metals.

## 1. Introduction

Present design practice for the fabrication of welded joints in AISI type 316 stainless steel requires that the as-deposited weld metal shall contain a 3 to 8% $\delta$-ferrite to prevent hot cracking during welding, and this may be achieved using a matching 316L composition of 19Cr–12Ni–3Mo.

Although the presence of the $\delta$-ferrite is essential to obtain the correct mechanical properties during welding, the inherent instability during service conditions produces a complex series of phase transformations [1, 2] which could have serious implications for both creep and fracture properties of the weld metal.

Previous work by Farrar and Thomas [2] on the phase transformations which occurred in 316L submerged arc weld metals after creep testing at 600° C, indicated that the $\delta$-ferrite transformation mechanism was highly complex. The transformation to $M_{23}C_6$ could occur at either the original $\delta$–$\gamma$ boundaries or within the $\delta$-ferrite laths depending upon the availability of suitable nucleation sites. The subsequent transformation to the intermetallic $\sigma$ phase depended upon the localized enrichment of chromium and molybdenum within the $\delta$-ferrite lath, and the proximity of the local composition to the ternary phase boundaries at 600° C.

The present work extends these studies with an investigation into the systematic microstructural and microcompositional changes which occur with ageing at 700° C of the original as-welded material.

## 2. Experimental details

Two weld metals which had displayed significantly different transformation kinetics were selected from previous studies [3]. These had been produced in the form of butt welds using a nominal heat input of 2.7 kJ mm$^{-1}$. The details of the consumables and the bulk analyses of these welds are given in Tables I and II respectively. Rods of 3 mm in diameter, were machined from the as-welded deposits for electron microscopy. The rods were encapsulated in evacuated silica capsules and aged at 700° C for 0.5, 5 and 100 h respectively, to produce material which had nominally transformed by 22, 53 and 100% (according to the equations calculated by Thomas and Yapp [4]). The samples were too small to be measured by the Magne–Gage technique.

After suitable slicing and mechanical polishing to 110 $\mu$m thickness, the discs were electropolished at 10° C in a solution of 10% perchloric acid in alcohol. Microstructural and microcompositional analyses were carried out on a JEOL 100 CX scanning transmission

0022–2461/85 $03.00 + .12 

TABLE I Combination of commercial fluxes, wires and welding conditions used

| Weld Number | Flux | Wire | A | V | Travel speed (mm min$^{-1}$) |
|---|---|---|---|---|---|
| 316-5 | Armco 880 | Oerlikon 316L | 400 | 34 | 305 |
| 316-6 | Armco ST100* | Oerlikon 316L | 400 | 34 | 305 |

*Indicates chromium compensating flux

electron microscope, STEM, fitted with an energy dispersive analyser, EDX. Typical micro-compositional analyses were carried out after accumulating 70 000–80 000 counts in 100 sec, giving a probable error of 0.25% in the calculated concentrations [5].

## 3. Results

### 3.1. Delta-ferrite phase transformation products

#### *3.1.1. Weld metal 316-5*

In the as-welded condition, the typical form of the $\delta$-ferrite is illustrated in Fig. 1. Detailed examination of the fringe contrast at the $\delta$–$\gamma$ boundaries revealed slight evidence of precipitation. Electron diffraction proved difficult and although no conclusive evidence as to their exact nature could be obtained, it may be presumed that the precipitation was an early stage of $M_{23}C_6$ development. After ageing for 0.5 h, distinctive changes were seen to occur both at the $\delta$–$\gamma$ boundaries and within the $\delta$-ferrite laths. In some laths large carbides developed profusely along the $\delta$–$\gamma$ boundaries, Fig. 2, whereas in others, carbides associated with dislocations were formed, Fig. 3. Electron diffraction evidence confirmed that both these precipitates were $M_{23}C_6$ carbides similar to those reported by Lai and Haigh [6].

Ageing for 5 h, appeared to allow the lath boundary carbides to grow and develop, Fig. 4, and to produce a complex transformation within the laths. In some there was evidence of the $\sigma$ phase and very small quantities of $\chi$-phase nucleating, Fig. 4, whereas in others the carbides associated with the dislocations had continued to develop, Fig. 5. There was also some evidence, Fig. 5, of the $\delta$–$\gamma$ boundary migrating away from the original position to leave isolated $M_{23}C_6$ carbides.

Finally, ageing for 100 h allowed the transformation to proceed to a mixture of intermetallic $\sigma$, $M_{23}C_6$ carbides and a little remaining $\delta$-ferrite.

Fig. 6 illustrates the complex mixture of $\sigma$ and $M_{23}C_6$ carbides which have replaced original $\delta$-ferrite; the carbide network in the latter being highly reminiscent of a eutectoid type of decomposition. In other laths, the transformation was incomplete and there was clear evidence of $\delta$-ferrite co-existing with $\sigma$ phase and partially spheroidized boundary carbides, Figs. 7 and 8. It is interesting to notice the fringe effects around the $\delta$-ferrite in Fig. 8, which are similar to those seen in the as-welded sample, Fig. 1.

#### *3.1.2. Weld metal 316-6*

In the as-welded condition, there was evidence of very small carbides at the $\delta$–$\gamma$ boundaries, Fig. 9, similar to those found by previous authors [2]. A clear example of these carbides is shown in Fig. 10, where they appear to be growing along to the original $\delta$–$\gamma$ boundaries.

Ageing for 0.5 h at 700° C, allowed these grain boundary carbides to grow along the $\delta$–$\gamma$ boundaries, Fig. 11, but there was no evidence of the massive development as seen in the 316-5 weld metal. In other laths where there was only limited carbide development, substantial transformation had taken place to $\sigma$ phase, Fig. 12.

After 5 h ageing, there was considerable formation of the $\sigma$ phase which now accounted

TABLE II Chemical analyses of parent plate and weld metals

| Element wt % | C | S | Mn | P | Si | B | Ni | Cr | Mo | Schaeffler Cr equivalent | Schaeffler Ni equivalent | As-welded % $\delta$-Ferrite |
|---|---|---|---|---|---|---|---|---|---|---|---|---|
| Parent plate | 0.024 | 0.021 | 1.47 | 0.017 | 0.38 | – | 11.2 | 17.0 | 2.42 | – | – | – |
| Weld 316-5 | 0.021 | 0.019 | 1.02 | 0.026 | 0.51 | 0.003 | 12.5 | 18.7 | 2.32 | 21.8 | 13.6 | 6 |
| Weld 316-6 | 0.026 | 0.019 | 1.48 | 0.030 | 0.57 | 0.004 | 12.0 | 19.5 | 2.27 | 22.6 | 13.5 | 12 |

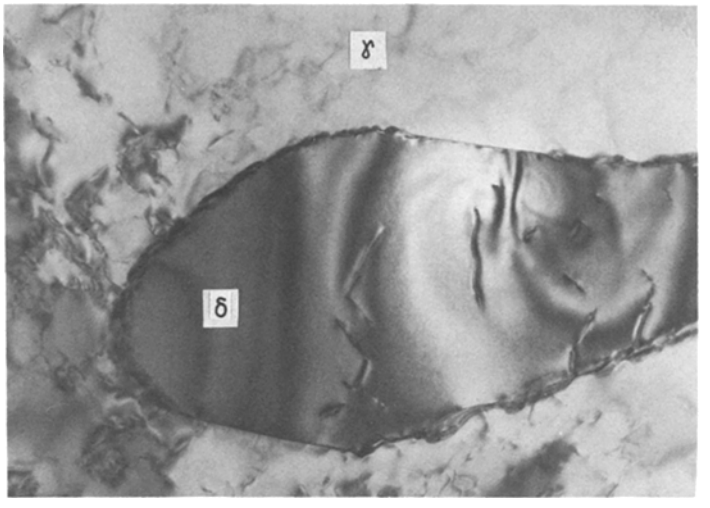


*Figure 1* A $\delta$-ferrite lath in the as-welded 316-5 material. Initial stages of carbide precipitation are evident at $\delta$–$\gamma$ boundaries. ( × 32 500).

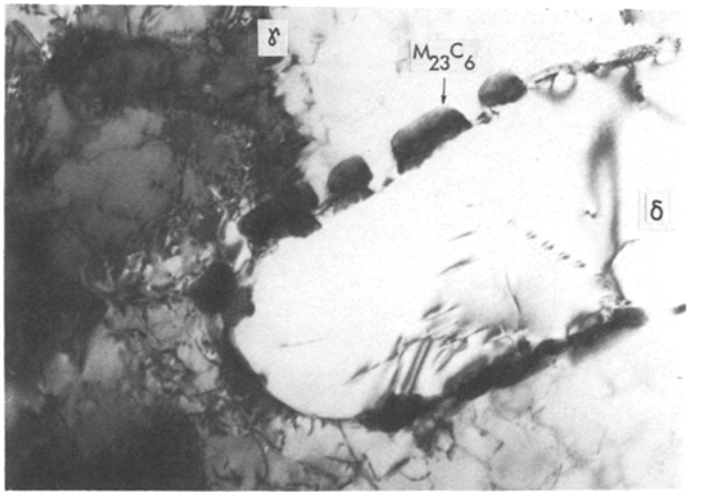


*Figure 2* Copious $M_{23}C_6$ precipitation at the $\delta$–$\gamma$ boundaries in 316-5 material aged for 0.5 h at 700° C. ( × 26 000).

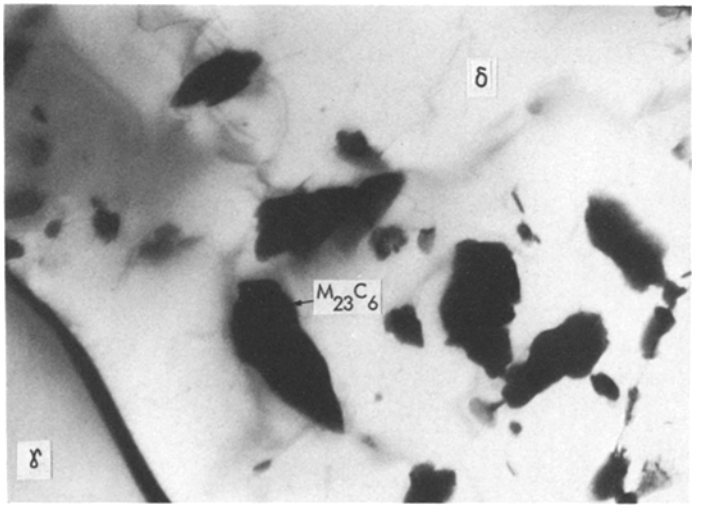


*Figure 3* Carbide precipitation associated with dislocation sites within a $\delta$-ferrite lath in 316-5 material aged for 0.5 h at 700° C. ( × 26 000).

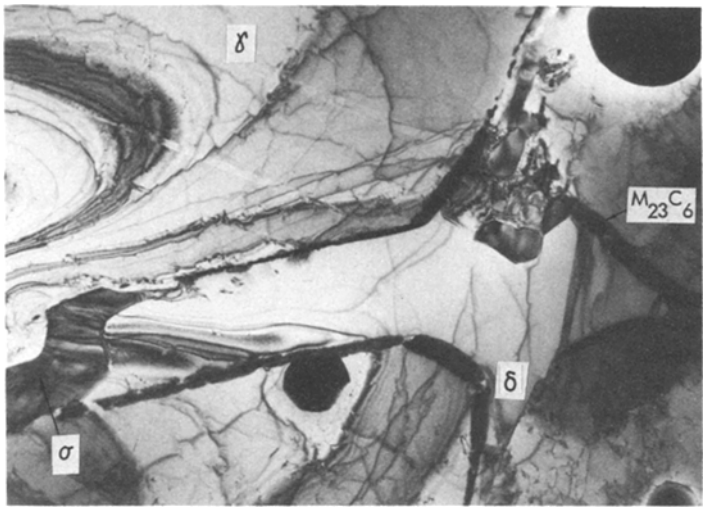


*Figure 4* Complex transformation to a mixture of carbides and intermetallic $\sigma$ phase in 316-5 material aged for 5 h at 700° C. (× 13 000).

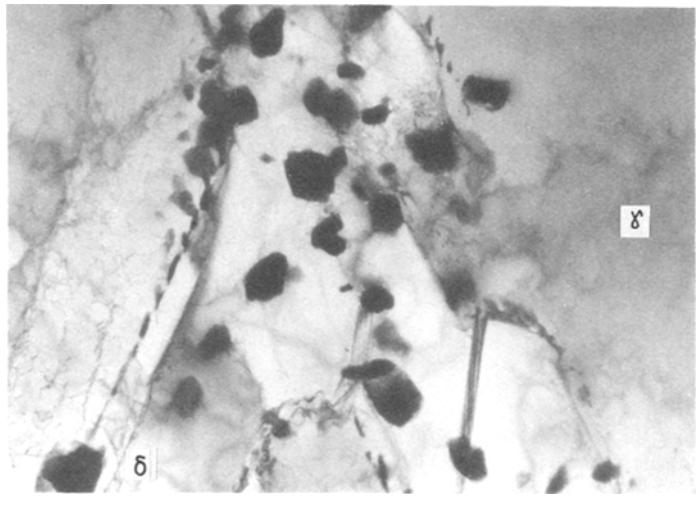


*Figure 5* Partial transformation to $M_{23}C_6$ carbides both at the $\delta$–$\gamma$ boundaries and within a $\delta$-ferrite lath in 316-5 material aged for 5 h at 700° C. (× 13 000).

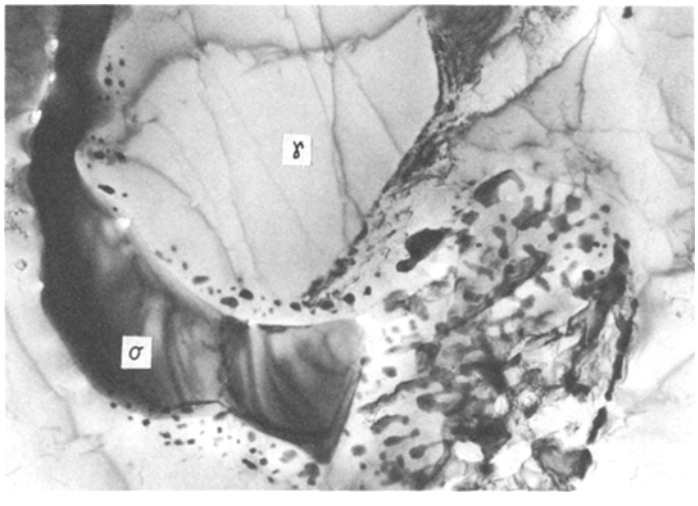


*Figure 6* Complete transformation of original ferrite to intermetallic $\sigma$ phase and a eutectoid like $M_{23}C_6$ carbide network in 316-5 material aged for 100 h at 700° C. (× 13 000).

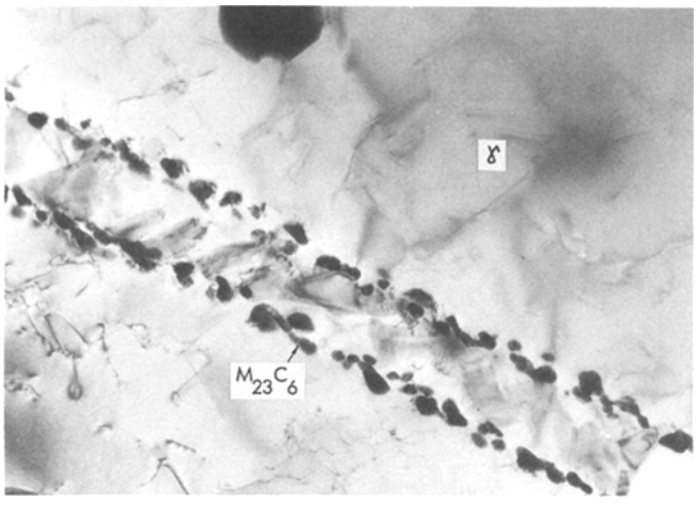


*Figure 7* Complete transformation of an original ferrite lath to austenite and $M_{23}C_6$ carbides in 316-5 material aged for 100 h at 700° C. ( × 26 000).

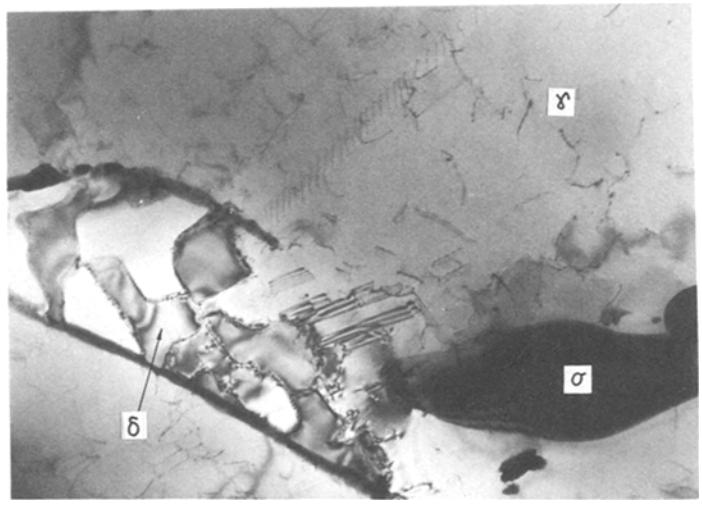


*Figure 8* Partial transformation of the $\delta$-ferrite to a mixture of $\sigma$ phase and carbides. Some stable $\delta$-ferrite remaining in 316-5 material aged for 100 h at 700° C. ( × 20 800).

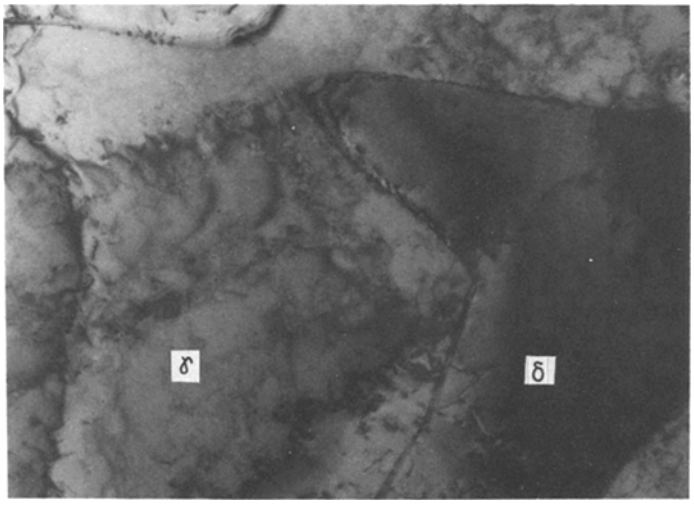


*Figure 9* A $\delta$-ferrite lath in as welded 316-6 material. ( × 26 000).

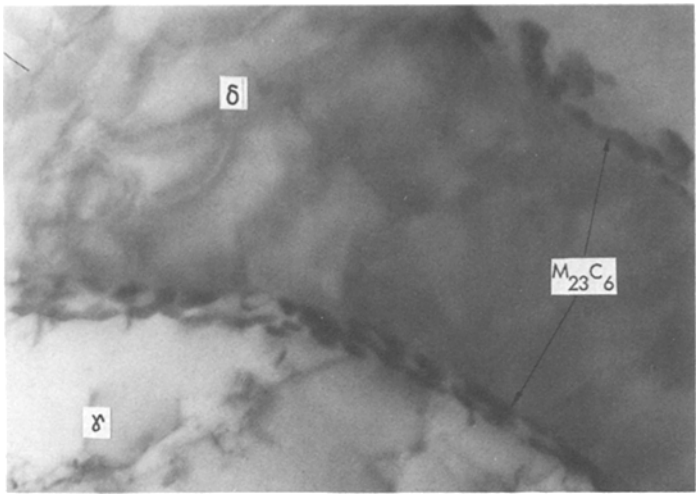


*Figure 10* Early stages of $M_{23}C_6$ precipitation at the $\delta$–$\gamma$ boundaries in as-welded 316-6 material. ( × 84 500).

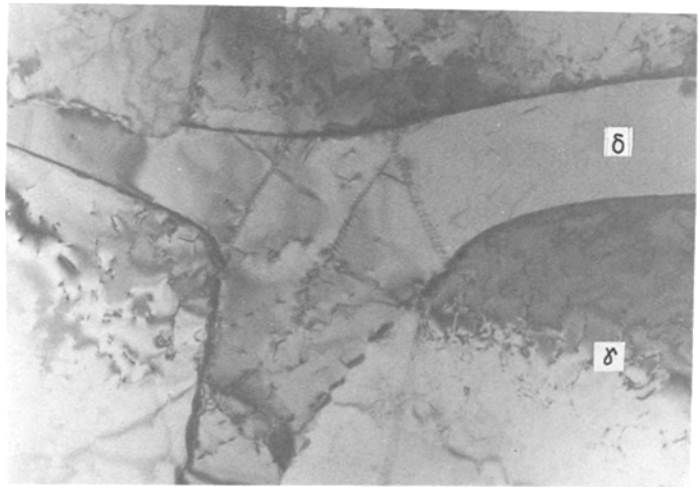


*Figure 11* Very limited carbide precipitation at the $\delta$–$\gamma$ boundaries compared to the situation shown in Fig. 2. 316-6 material aged for 0.5 h at 700° C. ( × 26 000).

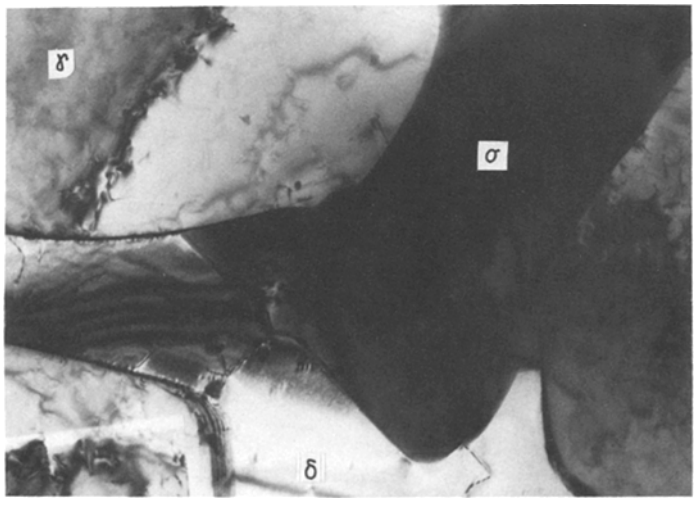


*Figure 12* Substantial transformation of original ferrite to intermetallic $\sigma$ phase in 316-6 material aged for 0.5 h at 700° C. ( × 26 000).

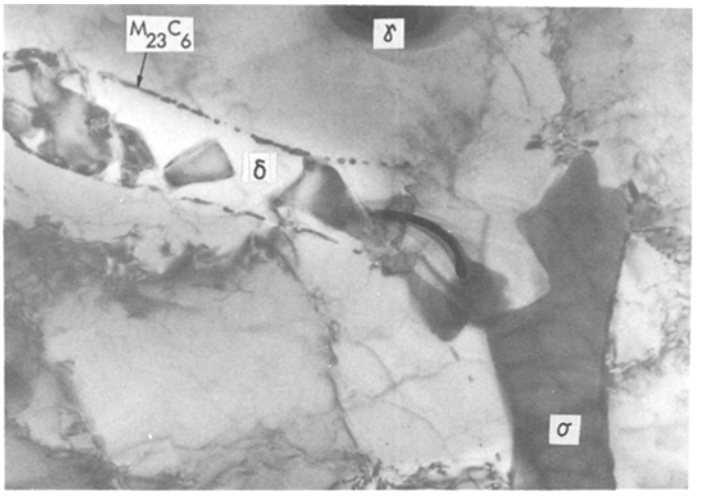


*Figure 13* Complex transformation to a mixture of intermetallic $\sigma$ phase and carbides in 316-6 material aged for 5 h at 700° C. (× 26 000).

for some 50% of the original $\delta$-ferrite laths, Fig. 13. The carbides at the $\delta$–$\gamma$ boundaries appeared to be breaking up and spherodizing, and the austenite boundaries had migrated from their original positions, Fig. 14.

Compared to the 316–5 weld metal, little or no evidence was seen of carbides associated with dislocations within the laths at any stage of the ageing sequence. 100 h ageing at 700° C, produced a complete transformation of the remaining $\delta$-ferrite to $\sigma$ phase. Clear diffraction patterns were obtained which frequently followed the orientation relationship

$$(1\,1\,1)\gamma \parallel (0\,0\,1)\sigma$$
$$\langle 0\,1\,1\rangle\gamma \parallel \langle 1\,4\,0\rangle\sigma$$

with lattice parameters $a_0 = 0.882 \pm 0.002$ nm and $c_0 = 0.433 \pm 0.002$ nm, these are similar to those reported by Weiss and Stickler [1]. Little evidence was obtained for any of the other intermetallic phases such as $\chi$ or R which have been reported by previous workers [6, 7]. The $M_{23}C_6$ carbides had become completely divorced from the $\gamma$–$\sigma$ boundaries, Figs. 15 and 16, and there was evidence that the spheroidized precipitates were beginning to redissolve as suggested by Thomas and Keown [8].

## 3.2. Microcompositional profiles

Following the previous work of Farrar and Thomas [2] which had revealed significant differences in the localized segregation of chromium, nickel and molybdenum in the $\delta$-ferrite, the present work studied the changing concentration of these elements with ageing at 700° C.

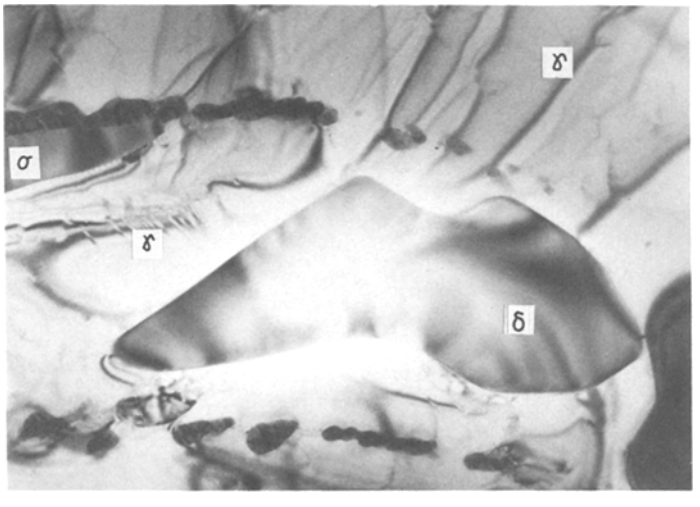


*Figure 14* Partial spheroidization of $M_{23}C_6$ carbides and migration of the $\delta$–$\gamma$ boundary from the original position as defined by the carbides in 316-6 material aged for 5 h at 700° C. (× 65 000).

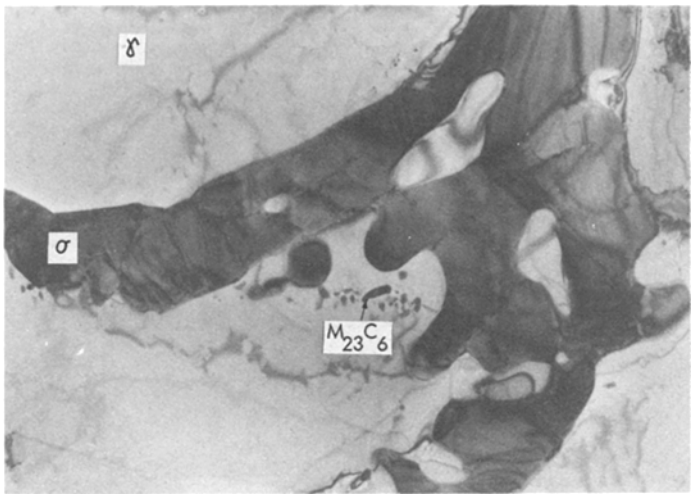


*Figure 15* Complete transformation to intermetallic $\sigma$ phase, together with spheroidization of the carbides at the original $\delta$–$\gamma$ boundary. 316-6 material aged for 100 h at 700° C. (× 10 400).

Figs. 17 and 18 illustrate the STEM/EDX segregation profiles of chromium, nickel and molybdenum in weld 316-5 in the as-welded and aged for 5 h-conditions. (The raw data was corrected using the $k$ factors reported by Farrar and Thomas [2].) The most significant feature revealed by these results was the incorporation of molybdenum into the grain boundary carbides, Fig. 18, with local values rising to 8 wt %. As there was some scatter in the analyses, the average of five different determinations for each material condition are plotted in Fig. 19. Significant changes in the molybdenum profiles are clearly evident. It is also interesting to notice that the chromium and nickel profiles did not alter significantly before 100 h ageing of the 316-5 weld metal. Similar results are presented in Figs. 20 to 22 for weld metal 316-6. In this material there was a slightly higher segregation of chromium, local values of 23 to 24 wt % were found in the as-welded condition compared with values of 21 to 23 wt % for the 316-5 material. However, there was less molybdenum, with local values of 3 wt % at the $\delta$–$\gamma$ boundaries. Fig. 22 indicates the systematic changes observed with ageing based on five different determinations for each material condition.

After 100 h ageing, the $\gamma$–$\delta$ boundaries as determined by the compositional profiles appear to have moved between 0.5 to 1.0 $\mu$m compared with the original position of the $\gamma$–$\delta$ boundaries, these being shown as dotted lines in Figs. 19 and 22.

If the shift in the profile is controlled by the diffusion of chromium in the austenite matrix, the mean shift, $\bar{x}$, may be calculated from the

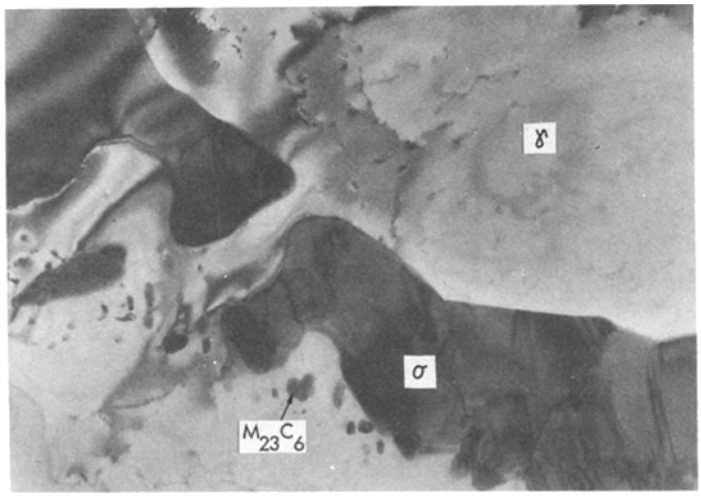


*Figure 16* Complete transformation of $\delta$-ferrite to intermetallic $\sigma$ phase. 316-6 material aged for 100 h at 700° C. (× 20 800).

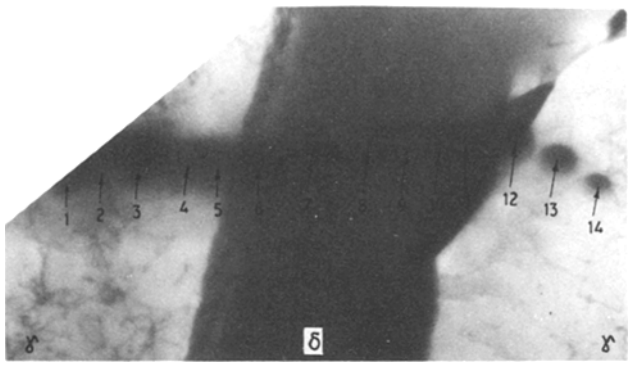


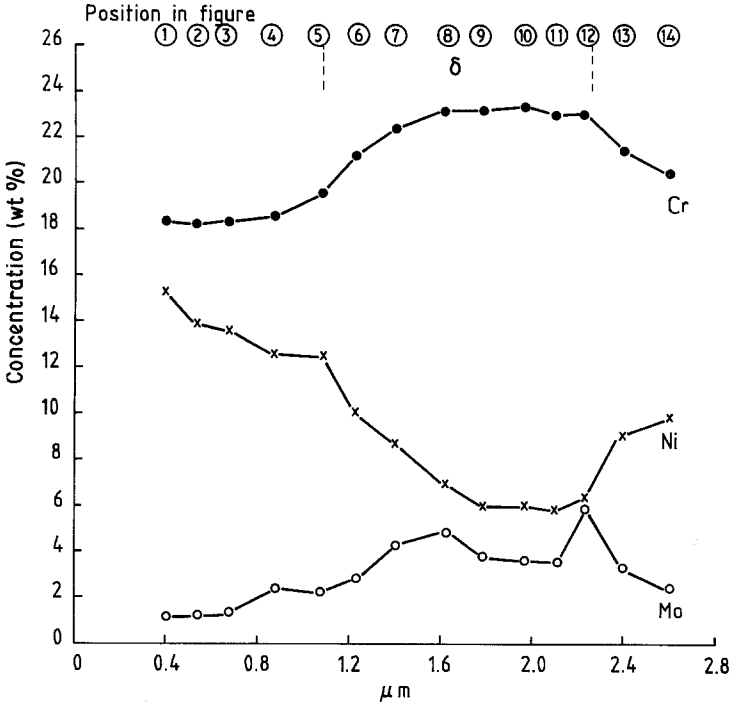


*Figure 17* Compositional profile across original $\delta$-ferrite lath in as-welded 316-5 material using STEM/EDX. (Foil thickness 270 nm).

error function expression, $\bar{x} \approx (Dt)^{1/2}$. Using $D = 5.7 \times 10^{-19}\,m^2\,sec^{-1}$ at 700° C [9], $\bar{x} \approx 0.45\,\mu m$ after 100 h, which is the same order of magnitude as the shifts observed.

## 4. Discussion

### 4.1. Influence of ternary Fe–Cr–Ni phase diagram

In an earlier study [3] of creep specimens tested at 600° C it was found that the measured transformation rates for welds 316-6 and 316-5 varied by factors of 2 to 3 faster and slower, respectively, compared with the rate predicted by Thomas and Yapp [4]. Considering the as-welded segregation analyses of chromium, nickel and molybdenum in the $\delta$-ferrite laths, it is clear from Figs. 19 and 22 that there are small, but significant differences between the two weld metals.

Plotting these analyses as Schaeffler chromium and nickel equivalents on the Fe–Cr–Ni phase diagram [10], it is apparent, Fig. 23, that the two welds lie in different areas of the equilibrium diagram.

Weld 316-5 lies on the phase boundary between the $\delta + \gamma + \sigma$ and $\sigma + \gamma$ phase fields. Since $\delta$ is a stable phase this would account for the slower transformation rates observed, as evidenced by the presence of untransformed $\delta$-ferrite after 100 h ageing at 700° C, Fig. 8.

Weld 316-6 lies within the $\sigma + \gamma$ phase field at 700° C, which is in agreement with the faster transformation rates and the microstructural

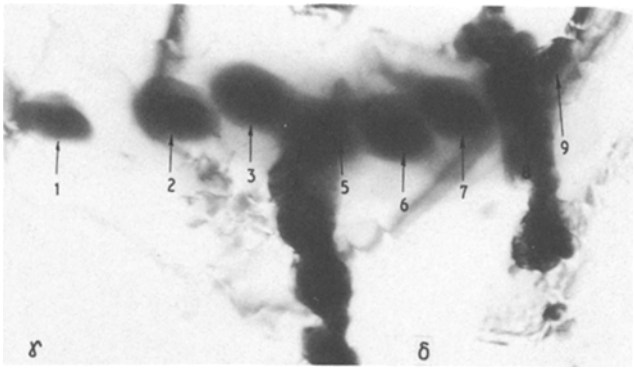


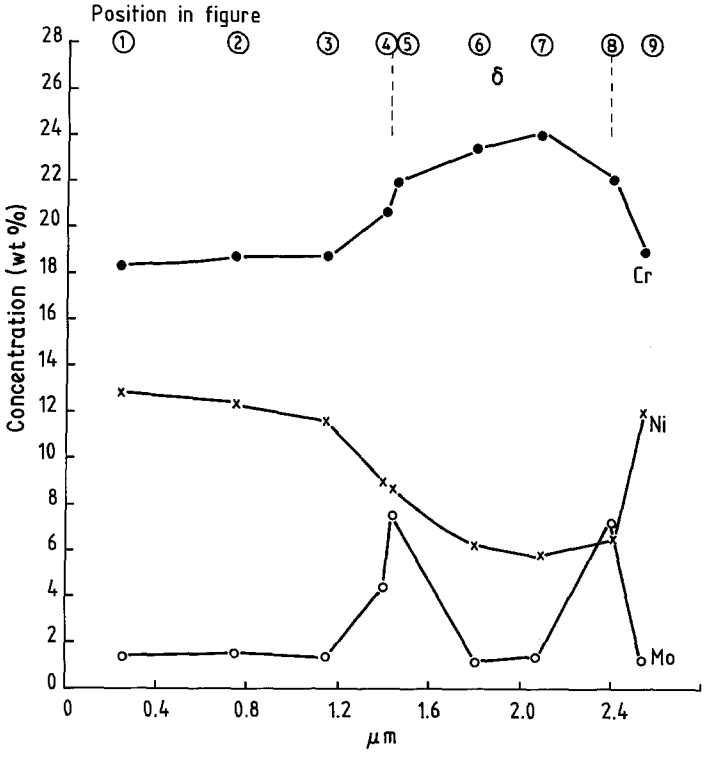


*Figure 18* Compositional profile using STEM/EDX across a partially transformed (nominal 53%) $\delta$-ferrite lath in 316-5 material aged 5 h at 700° C. Note the significant increase in molybdenum concentration at the $\delta$–$\gamma$ boundaries at points 4/5 and 8. (Foil thickness 240 nm).

evidence which indicated a complete transformation to the $\sigma$ phase after 100 h at 700° C.

As a question of the stability of the $\delta$-ferrite phase is under discussion here, it is useful to re-calculate the equivalent chromium and nickel concentration using the factors suggested by Irving *et al.* [1]. These produce small shifts on the ternary phase diagram from the points calculated using the Schaeffler equivalents, Fig. 23 but do not alter the final phases predicted.

As far as the co-existence of the $\delta$, $\gamma$ and intermetallic phases is concerned, it is felt that the use of the Fe–Cr–Ni ternary is more useful in this context than the Fe–Cr–Mo equilibrium diagram used by Slattery *et al.* [7], as the latter does not predict the presence of stable $\delta$-ferrite phase at the ageing temperature.

## 4.2. Transformation sequence for 19–12–3 materials

### *4.2.1. Previous work*

There have been numerous investigations into the phase transformations which occur in plate, cast and welded 316 materials when they are aged in the temperature range 600 to 900° C, and a summary of some of these results is presented in Table III.

Although these do not represent systematic studies relating the influence of as-welded composition and subsequent ageing temperature on

TABLE III Phase transformation products for aged 316 type materials

| Reference (material type) | Date | Material composition (wt %) | | | | | Original $\delta$-ferrite (%) | Transformation temperature (°C) | Observed phase reactions |
|---|---|---|---|---|---|---|---|---|---|
| | | C | Cr | Ni | Mo | Nb | | | |
| [5] (Cast material) | 1969 | 0.09 | 24.9 | 8.0 | – | – | 40 | 700<br>900 | $\delta \rightarrow M_{23}C_6 \rightarrow M_{23}C_6 + \sigma$<br>$\delta \rightarrow M_{23}C_6$ |
| [1] (Plate material) | 1972 | 0.02 | 17.3 | 13.1 | 2.7 | – | 0 | 600<br>700 | $\gamma \rightarrow M_{23}C_6 \rightarrow M_{23}C_6 + \eta$<br>$\gamma + M_{23}C_6 \rightarrow M_{23}C_6 + \eta + \chi$ |
| | | 0.07 | 17.4 | 12.3 | 2.1 | – | 0 | 600<br>700 | $\gamma \rightarrow M_{23}C_6 \rightarrow M_{23}C_6 + \eta$<br>$\gamma \rightarrow M_{23}C_6 \rightarrow M_{23}C_6 + \eta + \chi + \sigma$ |
| [6] (Weld material) | 1979 | 0.03 | 17.9 | 10.9 | 2.5 | – | 2–4 | 600<br>750<br>800 | $\delta \rightarrow M_{23}C_6 \rightarrow M_{23}C_6 + R + \sigma$<br>$\delta \rightarrow M_{23}C_6 \rightarrow M_{23}C_6 + \sigma$<br>$\delta \rightarrow M_{23}C_6 \rightarrow M_{23}C_6 + \chi + \sigma$ |
| [16] (Weld material) | 1980 | 0.04 | 17.1 | 10.8 | 2.3 | – | 6 | 850 | $\delta \rightarrow M_{23}C_6 \rightarrow M_{23}C_6 + \chi + \sigma$ |
| [14] (Plate material) | 1981 | 0.04–0.05 | 17.5 | 12.0 | 2.5 | – | 0 | 650 | $\gamma \rightarrow M_{23}C_6 + \eta + \sigma$ |
| [12] (Weld material) | 1981 | 0.1 | 18.8 | 8.1 | 3.4 | – | 18 | 650–750 | $\delta \rightarrow \sigma$<br>No electron microscopy was done and it is presumed that the initial $\delta \rightarrow M_{23}C_6$ reaction was missed |
| [15] (Weld material) | 1981 | 0.09 | 16.9 | 9.3 | 2.1 | – | 11 | 600 | $\delta \rightarrow M_{23}C_6 \rightarrow M_{23}C_6 + \chi$ |
| | | 0.03 | 18.7 | 12.4 | 2.7 | 0.6 | 5 | 600 | $\delta \rightarrow M_{23}C_6 \rightarrow M_{23}C_6 + \sigma + \chi$ |
| [13] (Cast material) | 1982 | 0.04 | 15.2 | 8.4 | 1.3 | – | ~4 | 649<br>732 | $\delta \rightarrow M_{23}C_6$<br>$\delta \rightarrow M_{23}C_6$ |
| | | 0.05 | 16.4 | 8.7 | 1.6 | – | ~5 | 649<br>732 | $\delta \rightarrow M_{23}C_6 \rightarrow M_{23}C_6 + \chi$<br>$\delta \rightarrow M_{23}C_6 \rightarrow M_{23}C_6 + \chi$ |
| [7] (Weld material) | 1982 | 0.07 | 18.0 | 8.9 | 1.9 | – | 6 | 625<br>850 | $\delta \rightarrow M_{23}C_6$<br>$\delta \rightarrow M_{23}C_6 \rightarrow M_{23}C_6 + \chi + \sigma$ |
| | | 0.05 | 20.5 | 10.1 | 3.1 | – | 18 | 625<br>850 | $\delta \rightarrow M_{23}C_6 \rightarrow \chi + \sigma$<br>$\delta \rightarrow M_{23}C_6 \rightarrow \chi + \sigma$ |

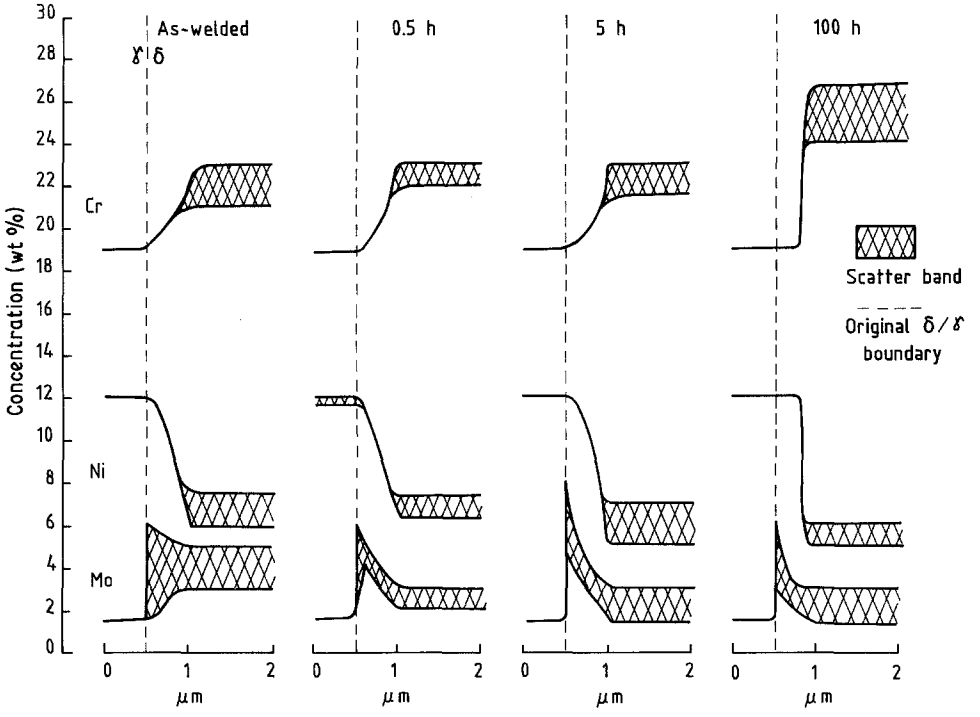


*Figure 19* Changes in the compositional profiles in the 316-5 material with ageing at 700° C. The curves represent the average of five readings at each ageing time and indicate the scatter of results obtained. The dotted line marks the position of the original $\delta$–$\gamma$ boundary.

the formation of intermetallic phases, an inspection of this literature allows the following general conclusions to be drawn:

1. The initial transformation products in either the austenite matrix or associated with the $\delta$-ferrite laths are $M_{23}C_6$ carbides.
2. The formation of intermetallic phases such as $\sigma$ and $\chi$ are encouraged by high concentrations of chromium and molybdenum and by ageing temperatures above 650° C. This conclusion is particularly supported by the work of Wegrzyn and Klimpel [12] and Leitneker [13].
3. The Laves phase ($\eta$), $Fe_2Mo$, is not normally observed in aged duplex weld metals.
4. The effect of carbon is highly complex and depends on the levels of chromium and molybdenum segregated to the $\delta$-ferrite laths. It has been suggested that $\sigma$ phase formation can be controlled by the carbon plus nitrogen levels [13]. If these are sufficiently high they can remove chromium to the carbides at the $\delta$–$\gamma$ interface and stabilize the remaining $\delta$-ferrite.

### 4.2.2. Systematic ageing at 700° C

The results obtained in this present study appear to confirm the sequential transformation mechanism proposed by Farrar and Thomas [2]. This mechanism involved the initial precipitation of carbides at the original $\delta$–$\gamma$ boundaries, or within the laths, followed by transformation to intermetallic phases if the localized chromium and molybdenum concentrations are still at adequate levels.

Considering the present results in the light of this sequence, a schematic transformation model for both the weld metals studied can be drawn, as shown in Fig. 24.

In both cases the first reaction is the development of $M_{23}C_6$ carbides at the $\delta$–$\gamma$ boundaries, these already being present in the as-welded 316-6 material, presumably due to the slightly higher chromium and carbon contents compared with the 316-5 material.

In the early stages of ageing the grain boundary carbides grow by the diffusion of carbon from the austenite matrix coupled with the diffusion of chromium and molybdenum from the $\delta$-ferrite. The lower initial concentration of chromium in the 316-5 weld material means that the $M_{23}C_6$ carbides can also develop within the $\delta$-ferrite laths, Fig. 3, whereas the higher initial

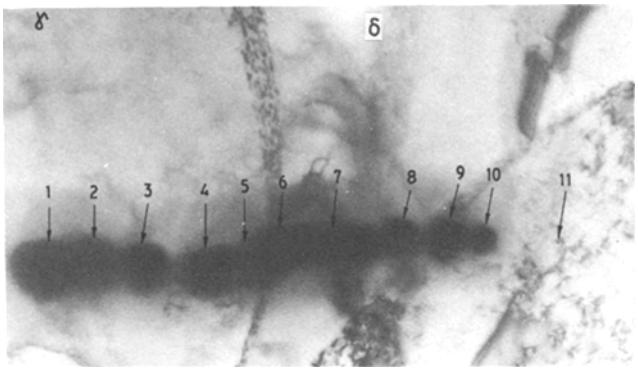


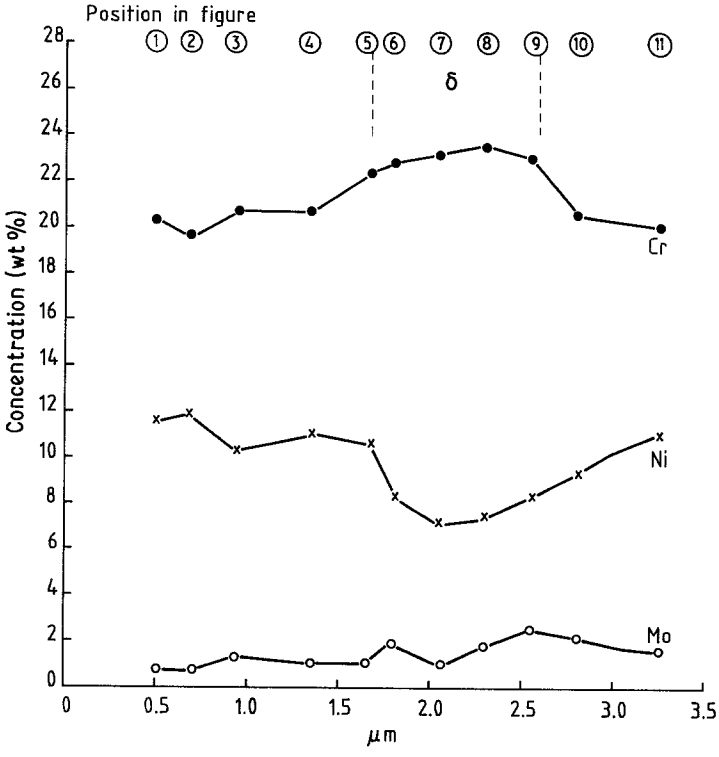


*Figure 20* Compositional profile across original $\delta$-ferrite lath in as-welded 316-6 material using STEM/EDX. (Foil thickness 253 nm).

concentration of chromium in the 316-6 weld metal allows intermetallic $\sigma$ phase formation, Fig. 12. With increasing ageing time, the difference between the two weld metals becomes more apparent. In the case of the 316-5 material, the remaining $\delta$-ferrite does not contain sufficient chromium and molybdenum to allow substantial $\sigma$ or $\chi$ phase formation, and the carbides continue to develop within the $\delta$-ferrite laths, Fig. 5. At this stage of the ageing sequence the original ferrite at the $\delta$–$\gamma$ boundary is denuded sufficiently in chromium and molybdenum to allow the $\delta$–$\gamma$ transformation to occur and the advancing $\gamma$ interface divorces the carbides, Fig. 14. After 100 h ageing, the phase transformation in weld 316-6 is complete with the remaining $\delta$-ferrite being converted to the $\sigma$ phase, Fig. 16. The $M_{23}C_6$ carbides are also disappearing due to the diffusion of chromium into the surrounding austenite matrix. In the case of weld 316-5, the lower chromium and molybdenum concentrations in the $\delta$-ferrite limits the transformation to $\sigma$ and some $\delta$-ferrite remains stable at 700° C, Fig. 8, the bulk of the $\delta$-ferrite having transformed to a complex $\gamma + M_{23}C_6$ network as illustrated in Fig. 6.

### 4.2.3. The role of the (chromium and molybdenum) equivalent

The work of Wegrzyn and Klimpel [12], Leitneker [13] and Slattery *et al.* [7], confirms the suggestions of Farrar and Thomas [2] that the

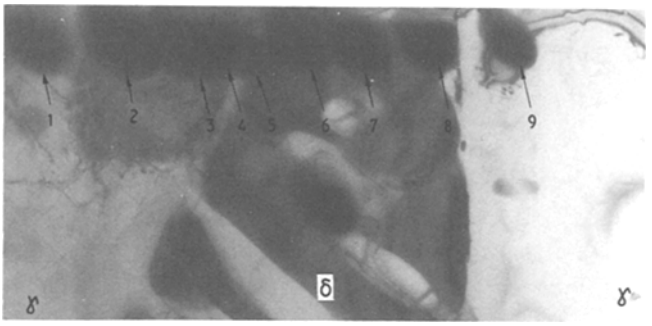


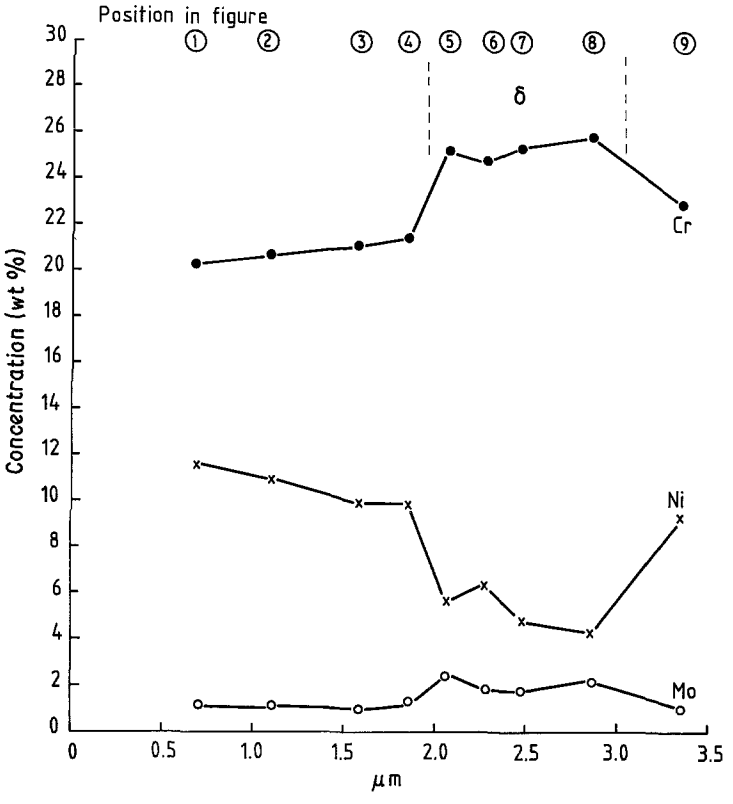


*Figure 21* Compositional profile using STEM/EDX across a partially transformed (nominal 53%) $\delta$-ferrite lath in 316-6 material aged for 5 h at 700° C. (Foil thickness 274 nm).

role of molybdenum is critical in determining the formation of intermetallic phases. If the original concentration of molybdenum in the $\delta$-ferrite is low, or if the $\delta$-ferrite becomes depleted in molybdenum, due to the precipitation of $M_{23}C_6$ carbides at the $\delta$–$\gamma$ boundaries, then intermetallic phase formation is severely retarded or even eliminated. Thus in weld 316-5, the copious precipitation of $M_{23}C_6$ carbides enriched in molybdenum, Figs. 5 and 18, has reduced the molybdenum concentration to 1.5 wt % and hence retarded $\sigma$ formation.

Finally it was found that the incorporation of molybdenum into the boundary carbides had led to the development of the $M_6C$ phase.

Weiss and Stickler [1] have suggested that this can occur by the reaction:

$$M_{23}C_6 \xrightarrow{+Mo} (Fe,Cr)_{21}Mo_2C_6 \xrightarrow{+Mo} M_6C$$

Electron diffraction evidence for this reaction was obtained in weld 316-5 after 100 h ageing at 700° C, this compares with 2000 h for fully austenitic materials [1]. It is difficult to separate the precise role of molybdenum from that of the chromium as both combine to enhance the formation of the $\delta$-ferrite in the as-welded material, but the present results seem to suggest that the removal of molybdenum from the $\delta$-ferrite has a more powerful effect on $\sigma$ phase formation than does chromium.

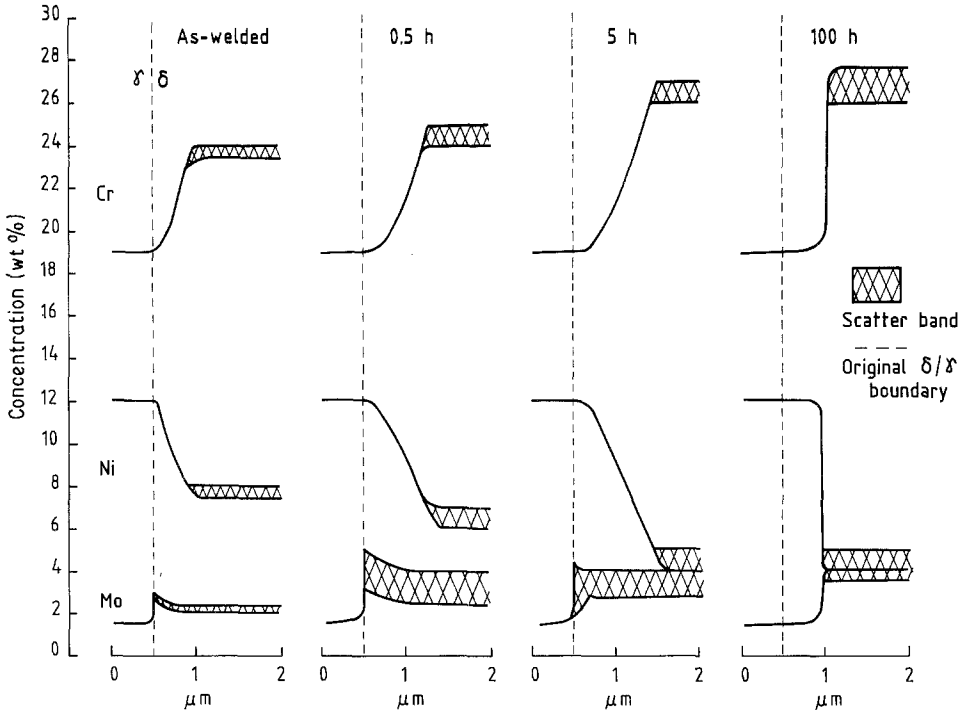


*Figure 22* Changes in the compositional profiles in the 316-6 material with ageing at 700° C. The curves represent the average of five readings at each ageing time and indicate the scatter of results obtained. The dotted line marks the position of the original $\delta$–$\gamma$ boundary.

## 4.3. Optimization of welding consumables

The different transformation rates and microstructural products observed in the two weld metals suggest that it might be possible to produce better long term stability at service temperatures in 19–12–3 weld materials.

It is suggested that adjustments in the carbon and molybdenum levels may be made to control intermetallic phase formation. If the carbon level were increased to ~0.04% and the molybdenum level reduced to ~2%, a lower propensity to intermetallic phase formation might be achieved in the 600 to 700° C regime by ensuring

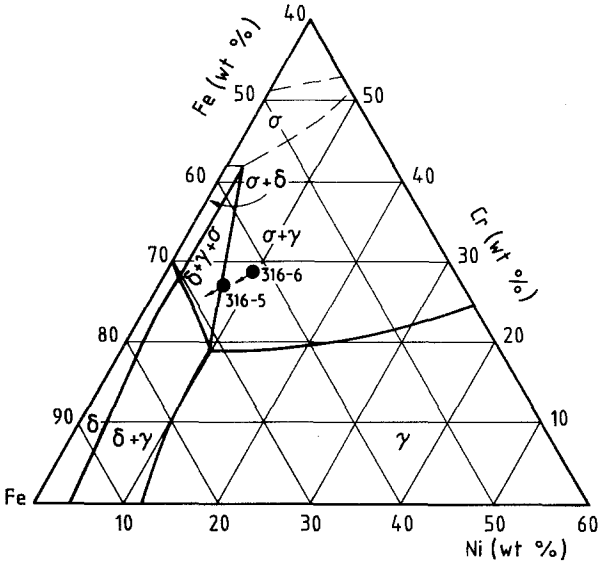


*Figure 23* 700° C isotherm of the Fe–Cr–Ni ternary system (after [10]) showing the composition, plotted as Schaeffler equivalents, of the as-welded $\delta$-ferrite (●). Shifts in the composition using the factors developed by Irving *et al.* [11] are shown as ●→.

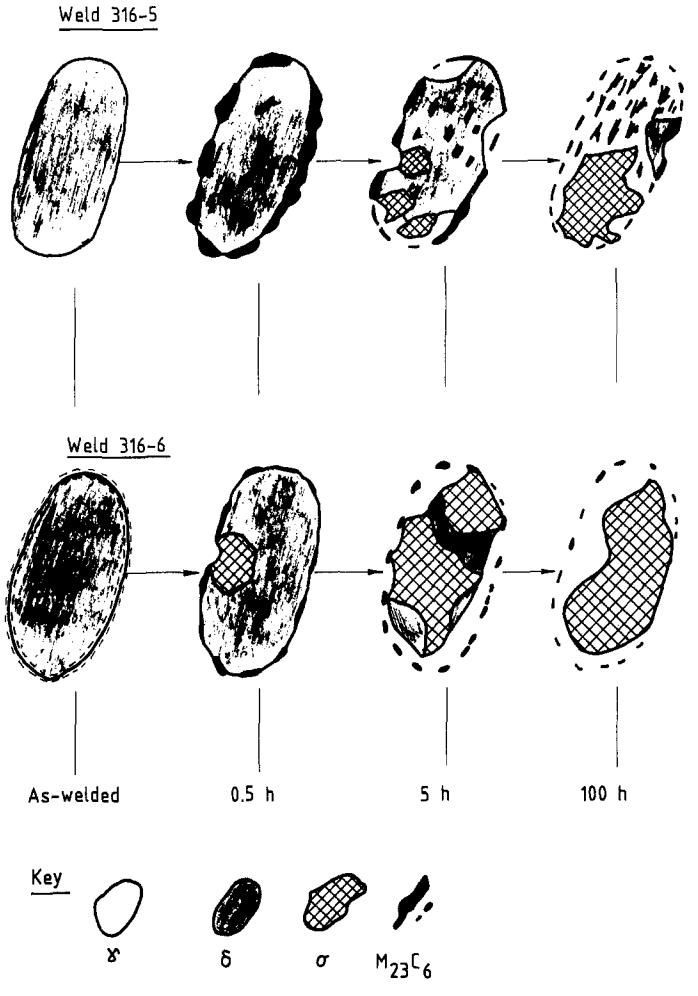


*Figure 24* Schematic $\delta$-ferrite transformation model for ageing at 700° C.

that only the $\delta \rightarrow M_{23}C_6$ reaction occurs at the $\delta$–$\gamma$ boundaries.

If the original segregation of chromium in the $\delta$-ferrite were also controlled by the use of non-compensating fluxes to produce leaner chromium deposits, it might be possible to achieve a longer term stability of the $\delta$-ferrite once the initial $\delta \rightarrow M_{23}C_6$ reaction has occurred.

A systematic series of studies on these small changes is required to determine the optimum composition for 316 duplex welds. Initial results by the current author using different manual metal arc rods with differing carbon levels appear to confirm this suggestion [17].

## 5. Conclusions

1. After ageing at 700° C, the original $\delta$-ferrite in the weld metals transforms to varying extents to mixtures of $M_{23}C_6$ carbides and $\sigma$ phase.

2. The rate of transformation of the $\delta$-ferrite depends on the original segregation of chromium, molybdenum and nickel in the as-welded condition.

3. The $\delta$-ferrite initially transforms to $M_{23}C_6$ carbides at the $\delta$–$\gamma$ boundaries or within the $\delta$-ferrite laths depending upon the availability of suitable nucleation sites.

4. If the initial segregation values allow the material to exist in the $\delta + \gamma + \sigma$ phase field at 700° C, the transformation is slow and the majority of the $\delta$-ferrite is converted to $\gamma + M_{23}C_6$, the balance of the $\delta$-ferrite remaining as a stable phase.

5. If the initial segregation values allow the material to exist in the $\gamma + \sigma$ phase field at 700° C the transformation is rapid and the majority of the $\delta$-ferrite is converted to $\gamma + \sigma$.

6. After the exhaustion of carbon within the $\gamma$ matrix, the austenite boundary migrates into the $\delta$-ferrite and the $M_{23}C_6$ carbides become divorced. At longer ageing times there was evidence that molybdenum was incorporated

into the boundary carbides and the transformation to $M_6C$ was occurring.

7. Suitable adjustments to the chromium, molybdenum and carbon contents should allow the development of a weld metal which has a very slow transformation rate at service temperatures, with the bulk of the transformation being to $M_{23}C_6$ at the original $\delta$–$\gamma$ boundaries.

## Acknowledgements

This work was carried out at the Marchwood Engineering Laboratories and the paper is published with the permission of the Central Electricity Generating Board. The author also wishes to acknowledge the continued interest of Dr R. G. Thomas, CEGB, Barnwood.

## References

1. B. WEISS and R. STICKLER, *Met. Trans.* **3** (1972) 851.
2. R. A. FARRAR and R. G. THOMAS, *J. Mater. Sci.* **18** (1982) 3461.
3. R. G. THOMAS, R. D. NICHOLSON and R. A. FARRAR, *Met. Technol.* **11** (1984) 61.
4. R. G. THOMAS and D. YAPP, *Weld. J. Res. Suppl.* **57** (1979) 361s.
5. F. R. BECKITT, *J. Iron Steel Inst.* **207** (1969) 632.
6. J. K. L. LAI and J. R. HAIGH, *Weld. J. Res. Suppl.* **58** (1979) 1s.
7. G. F. SLATTERY, M. E. LAMBERT and S. R. KEOWN, *Met. Technol.* **10** (1983) 373.
8. R. G. THOMAS and S. R. KEOWN, "Mechanical Behaviour and Nuclear Applications of Stainless Steels at Elevated Temperatures" Varese Conference May 1981 (Metal Society, London, 1982) Book 280, p. 30.
9. A. F. SMITH, *Metal. Sci.* **10** (1975) 375.
10. V. G. RIVLIN and G. V. RAYNOR, *Int. Met. Rev.* **248** (1980) 21.
11. K. J. IRVING, D. T. LLEWELLYN and F. B. PICKERING, *J. Iron Steel Inst.* **192** (1959) 218.
12. J. WEGRZYN and A. KLIMPEL, *Weld. J. Res. Suppl.* **60** (1981) 164s.
13. J. M. LEITNEKER, *ibid.* **62** (1982) 9s.
14. J. K. L. LAI, D. J. CHASTELL and P. E. J. FLEWITT, *Mater. Sci. Eng.* **49** (1981) 19.
15. R. G. THOMAS, (1981) CEGB Marchwood Engineering Laboratories Report RD/M/1191/R81.
16. G. F. SLATTERY and P. O'RIORDON, *Metallog.* **13** (1980) 59.
17. R. A. FARRAR, unpublished work (1985).

*Received 4 February*
*and accepted 13 March 1985*